Particle Production in pA Collisions at the LHC with QCD-based event-generator models

Klaus Geiger

Physics Department, Brookhaven National Laboratory, Upton, N.Y. 11973, U.S.A.

1 Theoretical approaches to a dynamical description

Within QCD phenomenology there exist basically two kinds of approaches to describe the evolution of high energy collisions involving nuclei, both of which have been extensively investigated in the past:

a) *String picture* [1, 2]: Based on phenomenological models of soft hadron-hadron interactions, the collision of a hadron with a nucleus is viewed as the projectile hadron's penetration and (multiple) scattering off nucleons in the nucleus. It is assumed that the hadron-nucleon scatterings are independent and involve only a small rapidity loss (of the order of one unit). The wounded nucleons draw color flux tubes (strings) between each other, and these strings subsequently fragment by $q\bar{q}$ production within a typical proper time of $\simeq 1\ fm$. The production of entropy and transverse energy is thus associated with non-perturbative, phenomenological string dynamics.

b) *Parton picture* [3, 4]: The description is founded on the fieldtheoretic parton picture of hadronic interactions within the firmly established framework of perturbative QCD. It attempts to calculate from first principles using renormlization-group improved evolution equations à la DGLAP. Both the colliding particles, hadron and nucleus, are visualized as clouds of quasireal quarks and gluons which penetrate through each other, leading to rapid materialization. Multiple short range scatterings between partons (minijet production) together with associated QCD radiation (gluon bremsstrahlung) produce the major part of the total entropy and transverse energy.

Clearly, both approaches have their conceptual problems and limitations. The *string picture* becomes questionable at very high collisions energies ($\sqrt{s}/A \gg 10\ GeV$) when the string density becomes large and the strings begin to overlap, so that they cannot be treated as individual entities that fragment independently. The *parton picture* on the other hand becomes doubtful at low beam energies ($\sqrt{s}/A \ll 100\ GeV$), where most parton scatterings involve momentum transfers too small to be described by perturbation theory, and where non-perturbative coherence effects of low-energy (small-x) partons break down the assumption of individual incoherent quanta. Loosely speaking, one may say that the *parton picture* is based on the explicit form of the QCD interaction between quarks and gluons, whereas on the other hand the string picture utilizes QCD terminology and the QCD degrees of freedom rather than the explicit form of the QCD Lagrangian.

In the context of collisions with nuclei, numerous Monte Carlo event generators that utilize the *string picture* have been developed over the years, for example, FRITIOF [5], VENUS [6], RQMD [7], DPM [8], QGSM [9]. Much fewer attempts have been made so far to simulate collisions involving nuclei at collider energies within the *parton picture*, i.e., on the level of microscopic parton dynamics. Currently there are only two such models on the market, namely, HIJING [10] and VNI [11]. The concept of VNI is to trace the real-time evolution of parton cascades in conjunction with a self-consistent hadronization scheme that is governed by the dynamics itself. The causal evolution from the initial state (e.g., hadron and nucleus) is followed by the time-development of the phase-space densities of partons, pre-hadronic parton clusters, and final-state hadrons, in position-space, momentum-space and color-space. The HIJING model also incorporates the perturbative QCD approach to multiple minijet production, however it does not incorporate a direct space-time description, and utilizes the aforementionend string-fragmentation approach, rather than a parton-cluster formation and decay, convert final-state partons into hadrons.

2 Space-time description of hadron-nucleus collisions in VNI

In the following, the approach implemented in VNI will be discussed briefly as an example to model hadron-nucleus collisions on the parton level, and to provide a useful, practical tool to estimate for instance the characteristic properties of particle production in these collisions. Details may be found in Ref. [11].

VNI, the parton-evolution is described in terms of a space-time generalization of the familiar momentum-space description of multipl (semi) hard interactions in QCD, involving $2 \rightarrow 2$ parton collisions, $2 \rightarrow 1$ parton fusion processes, and $1 \rightarrow 2$ radiation processes. The formation of color-singlet pre-hadronic clusters and their decays into hadrons, on the other hand, is treated by using a spatial criterion motivated by confinement and a non-perturbative model for hadronization. As advertized, the approach of VNI allows to study the time evolution of an initially prepared beam/target collision system in complete phase-space from the instant of collisional contact, through the QCD-evolution of parton distributions, up to the formation of final hadronic states. It provides a self-consistent scheme to solve the underlying equations of motion for the particle densities as determined by the microscopic dynamics.

A space-time description of multiparticle systems in high-energy QCD processes can be derived systematically from *quantum-kinetic theory* on the basis of QCD's first principles in a stepwise approximation scheme (see e.g., Refs. [12, 13] and references therein). Applied to the concept scetched in the preceeding subsection, this framework allows to cast the time evolution of the mixed system of individual partons, composite parton-clusters, and physical hadrons in terms of a closed set of integro-differential equations for the phase-space densities of the different particle excitations. The definition of these phase-space densities, denoted by F_α, where $\alpha \equiv p, c, h$ labels the species of partons, pre-hadronic clusters, or hadrons, respectively, is:

$$F_\alpha(r,k) \;\equiv\; F_\alpha(t,\vec{r};E,\vec{k}) \;=\; \frac{dN_\alpha(t)}{d^3r\,d^3k\,dE}\;, \tag{1}$$

where $k^2 = E^2 - \vec{k}^{\,2}$ can be off-shell or on-shell. The densities (1) measure the number of particles of type α at time t with position in $\vec{r} + d\vec{r}$, momentum in $\vec{k} + d\vec{k}$, and energy in $E + dE$ (or equivalently invariant mass in $k^2 + dk^2$). The F_α are the quantum analogues of the classical phase-space distributions, including both off-shell and on-shell particles, and hence contain the essential microscopic information required for a statistical description of the time evolution of a many-particle system in complete 7-dimensional phase-space d^3rd^3kdE, thereby providing the basis for calculating macroscopic observables. The phase-space densities (1) are determined by the self-consistent solutions of a set of *transport equations* (in space-time) coupled with renormalization-group-type *evolution equations* (in momentum space). (see Refs. [14, 12] for details). The practical solution of these fundamental equations is achieved by Monte Carlo simulation as implemented in VNI.

VNI as a whole consists of three major building-blocks:

1. The *initial state* associated with the incoming collision partners, that is, in the present context, hadron and nucleus. This involves the phenomenological construction of hadron and nucleus in terms of the partons' phase-space distributions on the basis of the experimentally measured hadron (nucleon) structure functions and elastic form-factors.

2. The *parton cascade development* with mutual- and self-interactions of the system of quarks and gluons. This includes multiple inelastic processes, described as sequences of elementary $2 \rightarrow 2$ scatterings, $1 \rightarrow 2$ emissions and $2 \rightarrow 1$ fusions. Moreover, correlations between primary virtual partons, emerging as unscathed remainders from the initial state, and secondary real partons, materialized or produced through the partonic interactions.

3. The *hadronization dynamics* of the evolving system in terms of parton-coalescence to color-neutral clusters as a local, statistical process that depends on the spatial separation and color of nearest-neighbor partons. Each pre-hadronic parton-cluster fragments through isotropic two-body decay into primary hadrons, according to the density of states, folowed by the decay of the latter into final stable hadrons.

Such a pragmatical division, which assumes complex interference between the different physics regimes to be negligible, is possible if the respective dynamical scales are such that the short-range (semi)hard parton interactions (scattering, radiation, fusion) of perturbative nature, and the non-perturbative mechanism of hadron formation (parton-coalescence and cluster-decay), occur on well-separated space-time scales (or momentum scales, by virtue of the uncertainty principle). Loosely speaking, the typical momentum scale associated with parton collisions, radiative emissions, or parton fusion, has to be larger than the inverse 'confinement length scale' $\sim 1\, fm$ which separates perturbative and non-perturbative domains. Further discussion of this condition of validity can be found in, e.g., [15, 16].

The program VNI is designed to provide a kinetic space-time description of parton evolution by utilizing well-developed techniques for perturbative QCD calculus in combination with

, and extending the application of this machinery from "clean" reactions (such as e^+e^-, ep, or pp collisions) this machinery to "dirty" collisions involving nuclei. Comparing VNI with the above-mentioned Monte Carlo models, the essential differences and partly new aspects are the following:

a) the aspects of the space-time evolution of the particle distributions in addition to the evolution in momentum space [15], and the concepts of quantum kinetic theory and statistical physics [12, 13].

b) the self-consistent interplay of coherent (angular ordered) perturbative parton evolution according to the DGLAP [17] equations, with the fully dynamical cluster-hadronization according to the phenomenological model of Ref. [14].

c) the microscopic tracing of color degrees of freedom and the effect of color-correlations by using explicit color-labels for each parton, which allows to investigate final state interactions in the process of hadron formation [18].

d) the diverse advantages of a stochastical simulation technique with which the various particle interaction processes are determined by the dynamics itself, through the local density of particles as they evolve causally in time.

e) the statistical many-particle description for general non-equilibrium systems, which allows to study thermodynamic behaviour of the bulk matter [19], such as the evolution of macroscopic energy density, pressure, etc., or the dynamical development of the sytem to thermal/chemical equilibrium in heavy ion reactions.

3 Examples of simulation results for pA collisions at the LHC

A systematic study of pA collisions in comparison with pp or $p\bar{p}$ collisions at the same energies is essential to gain insight into the importance of the medium effects due the nuclear environment of parton propagation and interaction, as well as on hadron production (e.g., shadowing, energy loss, brems-strahlung suppression, jet quenching, or $p_\perp$-broadening). Such effects are absent in pp ($p\bar{p}$) collisions, but become increasingly prominent in pA collisions, and are of major importance in AA reactions. Hence, by increasing the target mass A and the collider beam energy $\sqrt{s}$ in pA collisions, one may probe nuclear matter as a function of its density and study the gradually growing impact of medium and nuclear effects by comparing to pp collisions. Once the physics of 'QCD in medium' is better understood, then collective phenomena and medium effects in heavy ion collisions can be disentangled from the basic hadronic effects. Two interesting examples of how pA collisions may exhibit characteristic meduim effects, are discussed in the following, namely the issue of *parton saturation*, and the properties of *hadron production*

3.1 Parton saturation

In the parton picture a pA collision may be viewed as a diffusion of the partons of the projectile proton, traversing the nucleus and interacting frequently with partons belonging to different target nucleons [4, 20]. Multiple scattering and bremsstrahlung, accompanying the partons' paths through the nuclear medium, are expected to lead to a rapid entropy production that increases the local density and consequently enhance the probability for further interactions [15]. The fundamental question is, whether the intense parton multiplication that results in a dense phase-space population at small energy fractions $x \ll 1$, leads at some point to a probability larger than unity for a parton to interact with this dense parton matter, in which case the unitarity principle would be violated. This occurs when the partons are so densely packed that they

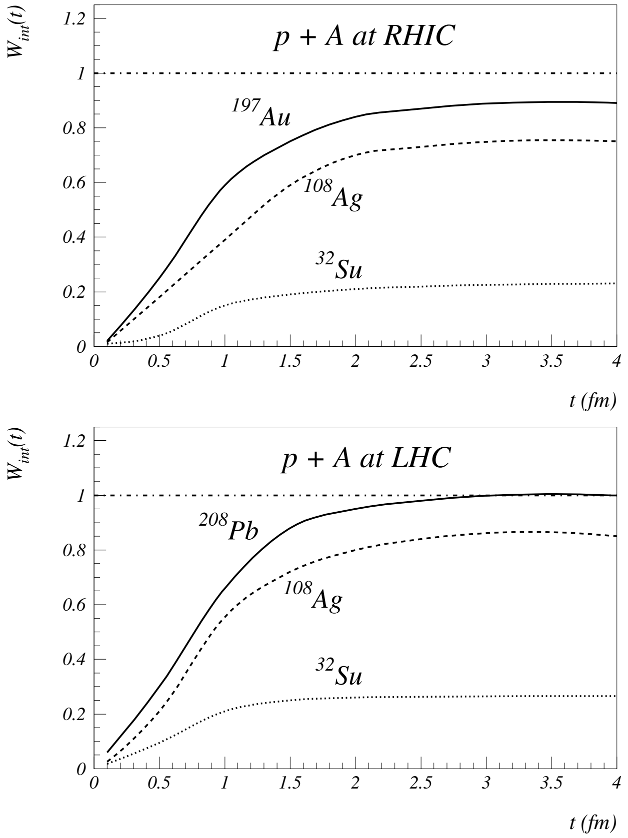

Figure 1: The phase-space integrated time evolution of the total parton interaction probability $W_{int} = \sum_a W_a$, where $W_a(p_a, \vec{r}, \Delta t) := \Delta t \sum_b \int_z^{z+\Delta z} dz \int_0^{R_A} d^2 r_\perp \; w_{ab}(p_a, \vec{r}, \Delta t)$ with $w_{ab}(p_a, \vec{r}, \Delta t) = \frac{1}{2E_a} \int \frac{d^3 p_b}{(2\pi)^3 2E_b} F_b(p_b, \vec{r}, t) \int \frac{d^3 p_c}{(2\pi)^3 E_c} \int \frac{d^3 p_d}{(2\pi)^3 E_d} \left[\sum |\mathcal{M}_{ab\to cd}|^2_{eff}(p_a, p_b, Q^2) \right] \delta^4(p_a + p_b - p_c - p_d)$.

spatially overlap in transverse direction and the nucleus appears to be completely black. However, detailed balance between scattering, branching and fusion processes must yield a local saturation of the parton density and stop a further increase, thereby ensuring unitarity. The requirement of unitarity conservation can be satisfied by demanding that the sum of probabilities of all elastic plus inelastic reaction channels must not exceed unity. When phrased in terms of the *Gribov-Levin-Ryskin unitarity condition* [4, 20]: the total interaction probability W_a of a given parton of species a to collide with another parton must always satisfy $W_a(t, \vec{r}) \le 1$ locally in space-time, where $a = g, q_f, \bar{q}_f$ labels the parton species.

In Fig. 1 the time evolution of the probability $W_{int} = \sum_a W_a$ at small rapidities $|y| \le 1.5$, obtained from the VNI simulations of pA collisions with various nuclei A at $\sqrt{s}/A \simeq 100$ GeV (RHIC) and $\sqrt{s}/A \simeq 7$ TeV (LHC). Common to both beam energies is that for light nuclei $A \lesssim 30$ the fusion probability is only $\simeq 0.2 - 0.3$, but it already reaches more than 70% for nuclei around $A = 100$, and 90 %, respectively 100 % for ^{197}Au at $\sqrt{s}/A = 100$ GeV (7 TeV). It is also interesting that the time it takes to increase W_g from 0.1 to 0.9 of its final value is typically a factor of 2 smaller at $\sqrt{s}/A = 7$ TeV than at $\sqrt{s}/A = 100$ GeV. Furthermore, at fixed $\sqrt{s}/A$ this time scale decreases significantly when proceeding from ^{32}S to ^{197}Au nuclei. Note that the saturating behaviour that is evident even for e. g. ^{32}S although W_g is far from unity, results from the fact that the duration of the reaction is the smaller the lighter the nucleus is, so that the partons naturally cease to interact (except for some small amount of residual interactions) when the system flows apart before it finally hadronizes.

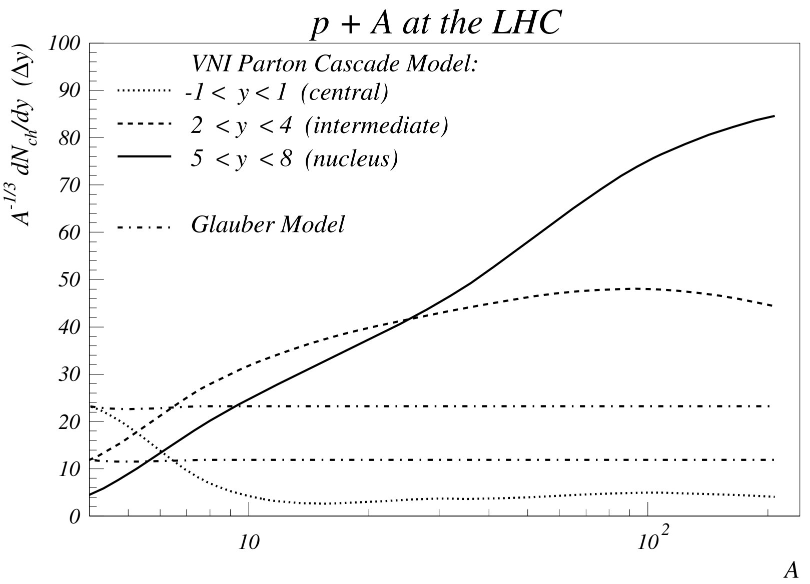

Figure 2: The mean multiplicity of charged particles $A^{-1/3}\, dN_{ch}/dy$ within different rapidity regions Δy, as estimated with the event generator VNI, and compared with naive expectations from the Glauber model.

3.2 Hadron production

As a second example, some properties of hadron production at LHC energy $\sqrt{s}/A \simeq 7$ TeV illustrate the outcome of the preceeding parton evolution and parton-hadron conversion via color-singlet coalescence.

In Fig. 2 the dependence of the multiplicity of produced charged particles on the the nuclear mass number A in different rapidity regions Δy is shown. The three curves differentiate the amount of particle production scaled by $A^{-1/3}$ in the central region $\Delta y = [-1, 1]$, the intermediate region $\Delta y = [2, 4]$, and the nucleus fragmentation region $\Delta y = [5, 8]$.

Finally, Fig. 3 depicts, in the top panel the rapidity distribution of charged particles in proton-lead collisions, whereas the bottom panel shows the average transverse momentum squared per particle as a function of Feynman-x.

It has to be emphasized that above considerations are rather qualitative at this point, and that it is most important to study and understand in detail nuclear and medium effects that give rise to the A-dependence as for instance in Figs. 2 and 3. Both theoretically and experimentally, the various mechanisms and their possible interference are to be addressed as a prime goal in the context of particle production. More accurate predictions will be calculable once these medium effects are better understood.

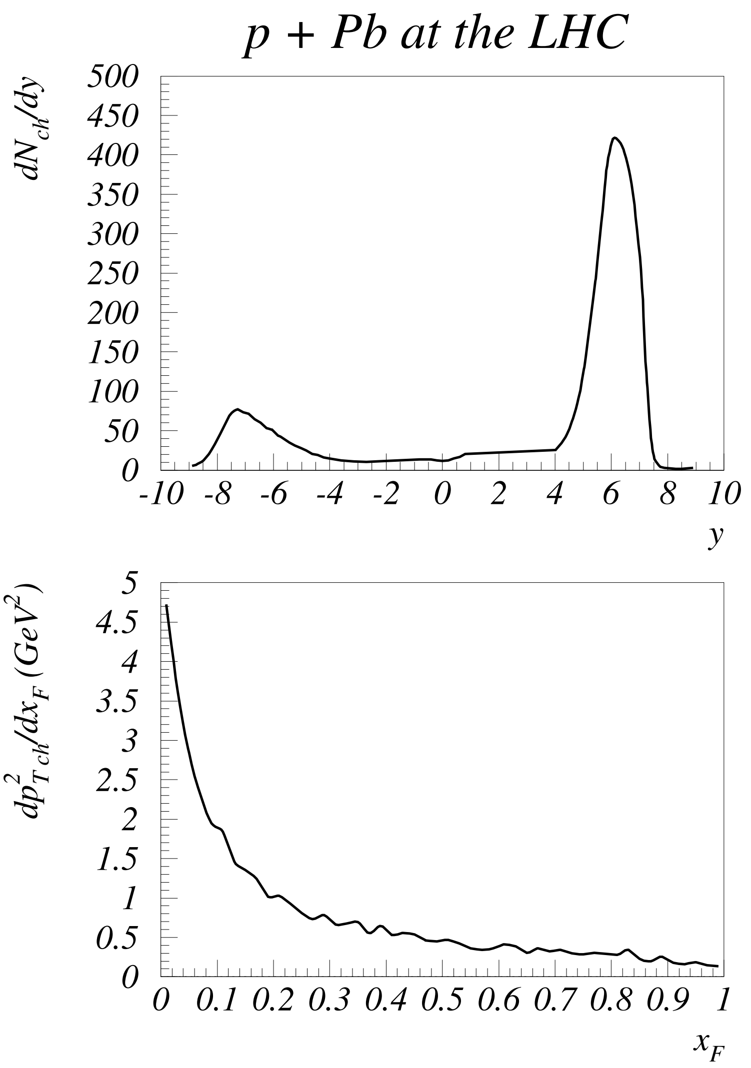

Figure 3: Particle spectra for $p + Pb$: top shows rapidity distribution dN_{ch}/dy, bottom shows average $p_{\perp ch}^2$ versus x_F, i.e., $dp_{\perp ch}^2/dx_F$.

References

[1] B. Andersson, G. Gustafson, G. Ingelman, and T. Sjöstrand, Phys. Rep. **97**, 33 (1983);

[2] B. Andersson, G. Gustafson and B. Söderberg, Nucl. Phys. **B264**, 29 (1986).

[3] Yu. L. Dokshitzer, D. I. Dyakonov, and S. I. Troyan, Phys. Rep. **58**, 269 (1980);

[4] L. V. Gribov, E. M. Levin, and M. G. Ryskin, Phys. Rep. **100**, 1 (1983).

[5] B. Andersson, G. Gustafson and B. Nilsson-Almquist, Nucl. Phys. **B281**, 289 (1987); B. Nilsson-Almquist and E. Stenlund, Computer Phys. Comm. **43** (1987), 387; B. Lörstad, Int. J. Mod. Phys. **A12**, 2861 (1989).

[6] K. Werner, Z. Phys. **C42**, 85 (1989); Phys. Rep. **232**, 87 (1993).

[7] H. Sorge, H. Stöcker, and W. Greiner, Nucl. Phys. **A498**, 567c (1989); Ann. Phys. **192**, 266 (1989).

[8] A. Capella, U. Sukhatme, C.-I. Tan, and J. Tran Tranh Van, Phys. Rep. **236**, 225 (1994)

[9] N. S. Amelin, E. F. Staubo, L. P. Csernai, V. D. Toneev, K. K. Gudima and D. Strottman, Phys. Rev. Lett. **67**, 1523 (1991).

[10] X. N. Wang and M. Gyulassy, Phys. Rev. **D44**, 3501 (1991); Comp. Phys. Com. **83**, 307 (1994).

[11] K. Geiger, preprint BNL-63632, hep-ph/9701226 (submitted to Comp. Phys. Com.).

[12] K. Geiger, Phys. Rev. **D54**, 949 (1996);

[13] K. Geiger, preprint BNL-63632, hep-ph/9611400.

[14] J. Ellis and K. Geiger, Phys. Rev. **D52**, 1500 (1995).

[15] K. Geiger, Phys. Rep. **258**, 238 (1995).

[16] *Basics of Perturbative QCD*, Advanced Series on

[17] L. N. Lipatov, Sov. J. Nucl. Phys. **20**, 94 (1975); Yu. L. Dokshitzer, Sov. Phys. JETP **46**, 641 (1977); G. Altarelli and G. Parisi, Nucl. Phys. **B126**, 298 (1977).

[18] J. Ellis and K. Geiger, Phys. Rev. **D54**, 1755 (1996).

[19] K. Geiger, Phys. Rev. **D46**, 4986 (1992).

[20] E. M. Levin and M. G. Ryskin, Nucl. Phys. **B304**, 805 (1989); Phys. Rep. **189**, 267 (1990).

[21] K. Geiger, Phys. Rev. **C49**, 3234 (1994).